Chemistry–A European Journal
Research Article
doi.org/10.1002/chem.202200227
Chemistry Europe
European Chemical Societies Publishing
www.chemeurj.org

The Role of Radical Bridges in Polynuclear Single-Molecule Magnets

Giang Truong Nguyen[a] and Liviu Ungur*[a]

Abstract: Employing radical bridges between anisotropic metal ions has been a viable route to achieve high-performance single-molecule magnets (SMMs). While the bridges have been mainly considered for their ability to promote exchange interactions, the crystal-field effect arising from them has not been taken into account explicitly. This lack of consideration may distort the understanding and limit the development of the entire family. To shed light on this aspect, herein we report a theoretical investigation of a series of N_2^{3-}-radical-bridged diterbium complexes. It is found that while promoting strong exchange coupling between the terbium ions, the N_2^{3-}-radical induces a crystal field that interferes *destructively* with that of the outer ligands, and thus reduces the overall SMM behavior. Based on the theoretical results, we conclude that the SMM behavior in this series could be further maximized if the crystal field of the outer ligands is designed to be *collinear* with that of the radical bridge. This conclusion can be generalized to all exchange-coupled SMMs.

Introduction

Single-molecule magnets (SMMs) are compounds that display magnetic hysteresis at the molecular scale.[1] They are promising candidates for future information storage,[2,3] spin qubit[4] and a variety of other spin-based devices.[5–10] However, their magnetic hysteresis is mostly observed at low temperature. In order to achieve any practical applications based on SMMs, the blocking temperature (T_B), whose definition is the highest temperature at which the hysteresis is observed, has to be raised significantly. For the last two decades, due to the intensive efforts of multidisciplinary research, T_B has been lifted from 2 K[2,11] to 80 K.[12]

Enhancing the exchange coupling between magnetic centers has been a promising approach to increase the blocking temperature.[13–19] It has been reported that the blocking energy barrier (U_{eff}) of lanthanide (Ln) complexes is proportional to the exchange coupling between the Ln ions.[20] The exchange coupling can be enhanced through a covalent metal-metal bond, which has been shown in several dimetallofullerenes (di-EMFs).[21–30] Among all di-EMFs, monolayers of $Tb_2@C_{80}(CH_2Ph)$ have shown the highest blocking temperature of 28 K.[31]

On the other hand, the exchange coupling can be promoted through a radical ligand bridging Ln ions. There are several radical-bridged dilanthanide complexes showing notable SMM behavior.[20,32–46] However, in 2016, a theoretical investigation of a series of N_2^{3-}-radical-bridged lanthanide complexes[47,48] indicated that the exchange from the radical bridge indeed decreases the SMM behavior of the complexes because the local crystal field (CF) of the Ln ions is not axial enough.[49] Following this work, in 2017, a series of complexes containing the same Ln^{3+}–N_2^{3-}–Ln^{3+} magnetic core was synthesized.[50] The outer ligands were substituted by cyclopentadienyl ligands (Cp), which have been well-known for the ability to deliver the strongest axial CF for oblate ions.[51] Nevertheless, it was shown last year that despite of using such ligands, the axiality and overall SMM performance of the complexes are only moderately improved.[52] Within the present computational investigation, we aim at shedding light on the origin of this discrepancy.

For this reason, it is of interest to evaluate the strength of the CF splitting induced by individual ligands in this N_2^{3-}-radical-bridged diterbium complexes and find their *individual* role for the magnetic axiality. To achieve that, ab initio calculations are performed on $[(Cp_2^{Me4H}Tb)_2(\mu\text{-}N_2^{\bullet 3-})]^-$ (Cp^{Me4H} = tetramethylcyclopentadienyl)[50] (**1-Tb**) (Figure 1(a)). The surrounding ligands are divided into two groups: the first group contains the Tb ion and two Cp ligands (denoted by **1-Cp**) (Figure 1(b)), while the second group contains the Tb ions and N_2^{3-} radical (denoted by **1-N**) (Figure 1(c)).

Results and Discussion

The CF of the Tb ions is described by the following Hamiltonian:[53]

$$\hat{H}_{CF} = \sum_{kq} B_k^q O_k^q(J), \tag{1}$$

where B_k^q is the CF parameters and $O_k^q(J)$ is the Steven operators of rank $k = 2, 4, 6$ and projection $|q| \leq k$. The computed CF parameters are illustrated in Table 1 while the CF splitting of the ground $J = 6$ multiplet is shown in Figure 2 and Table S1. It is noted that the two fragments **1-Cp** and **1-N** both generate

[a] G. T. Nguyen, Prof. Dr. L. Ungur
Department of Chemistry, Faculty of Science, National University of Singapore, Block S8 Level 3, 3 Science Drive 3 Singapore, Singapore 117543
E-mail: chmlu@nus.edu.sg

Supporting information for this article is available on the WWW under https://doi.org/10.1002/chem.202200227

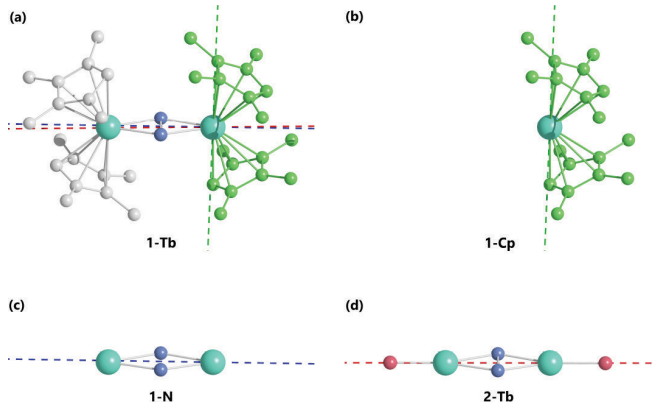

Figure 1. Molecular structures of (a) **1-Tb**, (b) **1-Cp**, (c) **1-N**, and (d) **2-Tb**. Red dashed line indicates the magnetic anisotropy axis while green and blue dashed lines are the directions of the CF of **1-Cp** and **1-N**, respectively. In (d), cyan, blue, and red spheres represent Tb, N and O atoms, respectively. Hydrogen atoms are omitted for clarity.

large CF splitting, even larger than the splitting of the entire **1-Tb** compound. Furthermore, the tunneling splitting (Δ_{tun}) within the ground Ising doublet is lower in both **1-Cp** and **1-N** compared to that of **1-Tb**. These results lead to the conclusion that the CF effects of both the ligand groups add up *destructively* for the magnetic axiality in the full compound. The analysis of the CF parameters in Table 1 indicates that the axial parameters of both **1-Cp** and **1-N** are dominant when they are written in the basis of their own local anisotropy axes. However, the CF parameters of **1-Cp** written in the coordinate system of the entire compound gives rise to many large nonaxial components, for example, e.g. $B_2^2, B_2^1, B_4^2, B_4^4$, etc. (the first column in Table 1) that certainly diminish the axiality of the entire **1-Tb** unit.

To explain this destructive effect of the Cp ligands, it is noted that the magnetic anisotropy axis of **1-Tb** is collinear with that of **1-N**. It is due to the fact that the CF strength exerted by the N_2^{3-} radical on the Tb ions is slightly stronger than that of the Cp ligands. The N_2^{3-} radical develops a larger electrostatic effect, due to a larger charge, as well as stronger covalent effects, due to a shorter chemical bond. The stronger CF effect of the radical can be viewed in the larger splitting of the ground $J = 6$ compared to that induced by the Cp ligands (Figure 2). In addition, according to the crystallographic information file of **1-Tb**,[50] the Tb–N bond lengths are around 2.22 Å that are much smaller than those between the Tb and C atoms in the Cp rings in **1-Cp** (2.65 Å to 2.77 Å). Thus, the anisotropy axis is expected to align towards the radical because the anisotropy axis of oblate ions is usually aligned towards the closest atom.[54] These rationalizations are also confirmed by the ab initio calculations (red dashed line in (Figure 1(a)). Hence, the N_2^{3-} radical is the dominant ligand defining the orientation of the anisotropy axis of the Tb centers. Since the two Cp ligands provide CF effect *perpendicular* to the magnetic anisotropy axis of the Tb ions (Figure 1), they diminish the

Table 1. Ab initio computed crystal-field parameters (B_k^q) and tunneling splitting within the ground CF Ising doublet (Δ_{tun}) for the two model fragments **1-Cp** and **1-N** and for the entire compound **1-Tb** and **2-Tb** in the coordinate system of the ground exchange state (red axis in Figure 1). The CF parameters of **1-Cp** in the coordinate system of its own ground anisotropy axis are illustrated for comparison.

k	q	1-Cp	1-Cp[a]	1-N	1-Tb	2-Tb
2	0	4.88	$-1.28\times10^{+1}$	$-1.14\times10^{+1}$	−9.16	$-2.71\times10^{+1}$
4	0	4.33×10^{-3}	1.18×10^{-2}	1.41×10^{-2}	8.76×10^{-3}	5.28×10^{-2}
6	0	2.20×10^{-5}	-3.70×10^{-5}	-6.24×10^{-5}	1.38×10^{-5}	-3.28×10^{-4}
2	−2	-9.11×10^{-1}	2.07	7.30×10^{-1}	2.91×10^{-1}	-1.73×10^{-2}
2	−1	9.30×10^{-1}	-1.01×10^{-1}	-1.07×10^{-1}	8.52×10^{-2}	6.50×10^{-4}
2	1	−3.22	5.31×10^{-2}	2.27	3.51×10^{-1}	9.41×10^{-1}
2	2	$-2.05\times10^{+1}$	-9.17×10^{-1}	$1.09\times10^{+1}$	−2.73	-9.10×10^{-1}
4	−4	4.94×10^{-3}	-4.52×10^{-4}	1.84×10^{-3}	5.41×10^{-3}	-3.39×10^{-4}
4	−3	-2.05×10^{-3}	3.76×10^{-3}	-9.81×10^{-4}	2.50×10^{-4}	2.41×10^{-4}
4	−2	-7.19×10^{-4}	-7.88×10^{-3}	-4.03×10^{-3}	-2.83×10^{-3}	-1.75×10^{-4}
4	−1	-1.04×10^{-3}	1.14×10^{-3}	-5.40×10^{-4}	-1.31×10^{-3}	-1.34×10^{-5}
4	1	-8.35×10^{-3}	-1.28×10^{-4}	-1.44×10^{-2}	-4.15×10^{-3}	-2.67×10^{-2}
4	2	-3.09×10^{-2}	3.34×10^{-3}	-6.51×10^{-2}	-1.39×10^{-2}	-2.74×10^{-2}
4	3	1.78×10^{-2}	4.49×10^{-3}	8.20×10^{-3}	1.13×10^{-2}	2.32×10^{-2}
4	4	4.60×10^{-2}	4.39×10^{-4}	1.36×10^{-2}	4.26×10^{-2}	-1.16×10^{-2}
6	−6	-1.15×10^{-5}	1.03×10^{-5}	2.77×10^{-6}	3.52×10^{-5}	1.15×10^{-5}
6	−5	-6.16×10^{-6}	6.39×10^{-5}	-7.32×10^{-6}	2.88×10^{-6}	-7.88×10^{-5}
6	−4	1.49×10^{-5}	-1.98×10^{-5}	-2.32×10^{-5}	-2.65×10^{-6}	-1.50×10^{-5}
6	−3	1.06×10^{-5}	-4.72×10^{-5}	4.73×10^{-6}	8.39×10^{-6}	-4.50×10^{-6}
6	−2	-1.71×10^{-5}	-1.16×10^{-6}	9.37×10^{-6}	1.39×10^{-5}	3.26×10^{-7}
6	1	-8.20×10^{-5}	-1.97×10^{-5}	1.88×10^{-4}	-3.10×10^{-6}	9.80×10^{-4}
6	2	-2.50×10^{-4}	1.69×10^{-5}	6.40×10^{-4}	-1.61×10^{-7}	9.51×10^{-4}
6	3	4.00×10^{-5}	-3.53×10^{-5}	-6.33×10^{-5}	-5.41×10^{-5}	-4.41×10^{-4}
6	4	2.27×10^{-4}	-5.88×10^{-5}	-1.72×10^{-4}	1.18×10^{-4}	-7.48×10^{-4}
6	5	-1.60×10^{-4}	-6.60×10^{-5}	5.69×10^{-5}	5.18×10^{-5}	-3.56×10^{-3}
6	6	1.90×10^{-5}	-1.54×10^{-5}	1.24×10^{-5}	3.56×10^{-4}	5.17×10^{-4}
		2.03×10^{-5}	2.03×10^{-5}	7.72×10^{-3}	4.93×10^{-2}	5.37×10^{-6}
	Δ_{tun}					

[a] The CF parameters of **1-Cp** quantized along its own local anisotropy axis (the green axis in Figure 1(b)).

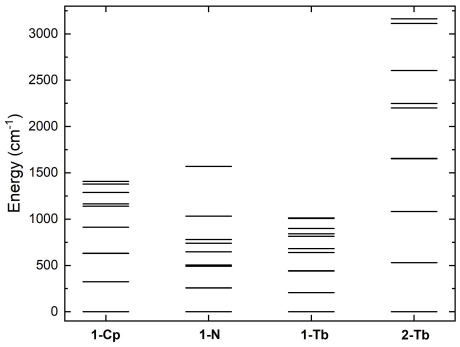

Figure 2. Calculated energies of the ground *J*-multiplet of the Tb ions (cm^{-1}).

magnetic axiality of the Tb ions and lower the performance of the whole complex.

Since the above CF analysis demonstrates that the CF perpendicular to the Tb^{3+}–N_2^{3-}–Tb^{3+} axis reduces the axiality, a promising alternative is to provide CF *parallel* to the axis. To testify this alternative, a hypothetical model $[(OTb)_2(\mu\text{-}N_2^{\bullet})]^-$ (**2-Tb**) (Figure 1(b)) is constructed in which each pair of the Cp ligands is substituted by an O^{2-} ion collinear with the Tb ions. We understand that such a model compound is not quite realistic in the chemical sense; however, we use it to exemplify the role of the collinearity in the CF generated by all the ligands. Based on the knowledge learnt from this model, some chemically feasible approaches to improve the SMM performance in this family are provided in the conclusion section.

The comparison between the CF parameters of **1-Tb** and **2-Tb** is illustrated in Table 1. Keeping the Tb–Tb axis as the main quantization axis, it is highlighted that the second rank axial CF parameter B_2^0 of **2-Tb** is nearly three times greater than that of **1-Tb**; the other axial parameters of the former are around an order of magnitude larger than the latter. Additionally, the nonaxial components of the former are much smaller than the latter. In Figure 2 and Table S1, the energy gap between the two lowest doublets in **2-Tb** is more than twice as large as in **1-Tb**; the total splitting within the ground *J*-multiplet of the former is also around threefold the latter. The tunneling gap in the ground doublet in **2-Tb** is reduced by nearly four orders of magnitude. Therefore, it is certain that by making the CF of the outer ligands *collinear* with the CF generated by the N_2^{3-} radical, the axiality of the Tb centers is drastically enhanced. In contrast with the Cp ligands in **1-Tb**, the O^{2-} ions in **2-Tb** provide CF parallel to that of the magnetic core; thus, both of them tend to align the anisotropy axis in the same direction. In other words, by this approach, the CF competition in **1-Tb** becomes the CF cooperation in **2-Tb**.

On the basis of the obtained CF states, the exchange levels are calculated by the following exchange model:[49,52,55]

$$\hat{H} = \hat{H}'_{CF} + \hat{H}_{ex}, \tag{2}$$

$$\hat{H}'_{CF} = \sum_{i=1,2}\sum_{k=2}^{6}\sum_{q}\mathcal{J}_{kq00}\frac{O_k^q(\hat{J}_i)\hat{I}}{O_k^0(J)}, \tag{3}$$

$$\hat{H}_{ex} = \sum_{i=1,2}\sum_{k=1}^{7}\sum_{q,q'}\mathcal{J}_{kq1q'}\frac{O_k^q(\hat{J}_i)\hat{S}_{q'}}{O_k^0(J)S}, \tag{4}$$

where $\hat{H}_{CF}{}'$ is the contribution to the local CF splitting arising from the electron delocalization between Ln^{3+} and N_2^{3-}, and $\hat{H}_{ex}$ describes the exchange interaction between them. The summation over $i = 1, 2$ represents the interaction between the Tb ions and the radical. $\mathcal{J}_{kq00}$ (even k) and $\mathcal{J}_{kq1q'}$ (odd k) are exchange parameters with rank k up to 7 and projection $|q|$ up to 5; $\hat{I}$ and $\hat{S}$ are the unit and spin operators of the radical, respectively; $O_k^q(\hat{J}_i)$ is the Steven operator.

The local CF states modified by $\hat{H}'_{CF}$ are given in Table S3. The calculated exchange levels are illustrated in Figure 3 and Table S4–S6. Interestingly, in **2-Tb**, the admixture between the ground and excited CF states in the four lowest exchange doublets is suppressed. Compared to **1-Tb**, the rate of quantum tunneling mechanism (QTM) in **2-Tb** is significantly reduced by eight orders of magnitude as the matrix element within the ground doublet in **2-Tb** is lowered by four orders of magnitude. The element connecting the ground and first-excited levels in **2-Tb** is also an order of magnitude smaller than in **1-Tb**. Therefore, at low temperature, the magnetization is expected to relax via the fourth level, doubling the blocking energy barrier via the first-excited one, owing to the exclusion of the CF excited states in the exchange admixture as predicted in Ref. [49]. On the other hand, the rate of temperature-assisted QTM between -7 and $+7$ states is in the same order of magnitude with that between -2 and $+2$. Hence, there may exist another relaxation path that is -1, -4, -6, -7 then to the other side of the diagram reaching to the blocking energy of more than 750 cm^{-1}.

Conclusion

In this work, based on the ab initio computational investigation of the N_2^{3-}-radical-bridged diterbium compounds, the interplay between the CF exerted by different ligand groups was analyzed. It was found that the N_2^{3-} radical exerts a strong CF effect on the Tb ions, even stronger than that of Cp ligands, forcing the ground-state magnetic anisotropy to be nearly collinear with the Tb^{3+}–N_2^{3-}–Tb^{3+} axis. Furthermore, the CF generated by Cp and N_2^{3-} ligands add up *destructively*, perturbing the magnetic axiality of the Tb centers. The reason for this is the nearly perpendicular alignment of these two ligand groups.

When the dominant CF effects of the outer ligands and of the bridging N_2^{3-} radical are made collinear, the on-site CF splitting of the ground *J*-mulitplet is strongly enhanced because of the addition of the axial parameters, while the QTM of the ground exchange doublet is suppressed due to the reduction of

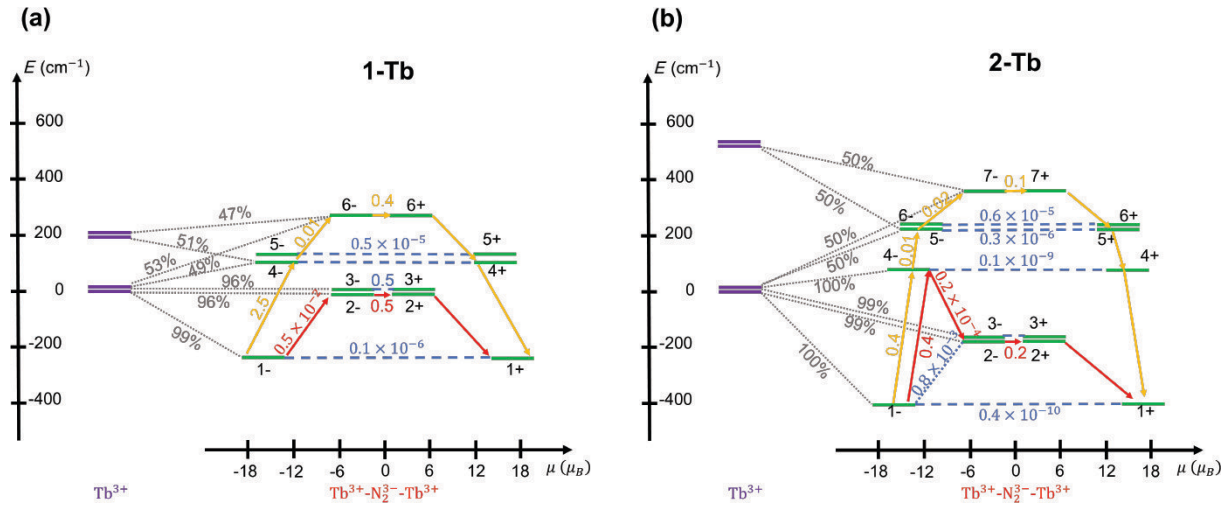

Figure 3. Magnetization blocking diagrams in (a) **1-Tb** and (b) **2-Tb**. Purple bands demonstrate CF doublets and green bands are exchange levels. Gray dotted lines with gray percentages show the admixture of the CF doublets to the exchange levels. Blue dashed lines represent the rate of the (temperature-assisted) quantum tunneling mechanism. Red and orange arrows indicate the first and second possible relaxation paths of magnetization, respectively. Blue and red numbers are the matrix elements of transition magnetic moment.

the nonaxial components. This conclusion can be generalized to all exchange-coupled SMMs.

For this particular Ln^{3+}–N_2^{3-}–Ln^{3+} series, two promising solutions to improve the SMM behavior are:

- to align the outer ligands so that their dominant CF effect is collinear with the Ln^{3+}–N_2^{3-}–Ln^{3+} axis,
- to replace the Cp ligands by other ligands, which hold a very weak CF effect, for example, N-bonded or I-bonded, preferably neutral. In this case, the dominant CF axiality will arise from the N_2^{3-} radical.

It is noteworthy that in the development of radical-bridged polynuclear SMMs, the radical has been mainly considered for its ability to promote exchange interactions. On the other hand, the CF effect arising from the radical has not been taken into account explicitly. It was shown in this work that the microscopic picture of the local CF of the Tb ions is not correctly interpreted unless the CF of the N_2^{3-} radical is considered. Therefore, in order to achieve better radical-bridged polynuclear SMMs in the future, not only the exchange strength but also the CF effect of the radical must be examined carefully.

Finally, it is predicted that the ultimate SMM performance of exchange-coupled compounds involving anisotropic ions linked by radicals could be obtained when the radicals induce CF collinear with the magnetic anisotropy axis while the magnetic exchange is *ferromagnetic*,[28,56] instead of the currently dominant antiferromagnetic. As an example, for this purpose, the energy of the magnetic orbital of the radical must be made in resonance with the 6 s/5d orbitals of the lanthanide (which are more diffuse and able to promote ferromagnetic exchange by making use of the high-spin (Hund) intermediate term in the electron transfer process), such that the Goodenough mechanism becomes operative.[57] Besides, the ferromagnetic configuration is favored by the dipolar magnetic coupling between collinear alignment of the local magnetic moments. To demonstrate this effect, a simulation of the exchange spectra of **2-Tb** using the Lines exchange model with ferromagnetic interaction $J = +20$ cm^{-1} shows a barrier height of more than 1200 cm^{-1} (see Figure S1). In addition, the advantage of ferromagnetic exchange and CF collinearity has been observed in some dimetallofullerenes.[30,58,59] Recently, a mixed-valence $(Cp^{iPr5})_2Dy_2I_3$ (Cp^{iPr5} = pentaisopropylcyclopentadienyl)) complex exhibiting both of the properties has set the record 100-s blocking temperature of 72 K.[60] Thus, the prediction in this work is strongly supported by these novel experimental results

Computational Methods

Ab initio calculations were performed in the MOLCAS 8.4 program.[61,62] The molecular structure of **1-Tb** was rotated and translated so that the exchange core possesses D_{2h} symmetry.[49] The Tb atom on the left was substituted by the analogous Lu^{3+} ion. The ANO-RCC-VTZP basis sets[63] were employed for all the atoms. A point charge of −0.5 *e* was placed on each N atom to mimic the electrostatic effect from the unpaired electron in the N_2^{3-} radical. Spin-free wavefunctions were computed in the CASSCF module with the active space consisting of 8 electrons in 7 4*f* orbitals. Subsequently, the spin-orbit coupling was included in the RASSI module[64] mixing the full energy spectrum of Tb^{3+} ion, that is, 7 septet, 140 quintet, 588 triplet, 490 singlet states. Based on the spin-orbit wavefunctions, the CF parameters and energy levels of the ground *J*-multiplet were calculated by using the SINGLE_ANISO module.[65–68] Finally, the exchange interaction is taken into account by means of the superexchange model[49] which has been implemented in the POLY_ANISO module.[67,69]

Acknowledgements

L.U. acknowledges the financial support of the research projects R-143-000-A65-133, R-143-000-A80-114 and A-8000017-00-00 of

the National University of Singapore. Ab initio calculations were done on the ASPIRE-1 cluster (www.nscc.sg) under the project 11001278. G. T. N. was supported by the NUS Research Scholarship program.

Conflict of Interest

The authors declare no conflict of interest.

Data Availability Statement

The data that support the findings of this study are available in the supplementary material of this article.

Keywords: ab initio calculations · crystal-field theory · exchange interaction · quantum chemistry · single-molecule magnets

[1] D. Gatteschi, R. Sessoli, J. Villain, *Molecular Nanomagnets*, Oxford University Press, Oxford, 2006.
[2] R. Sessoli, D. Gatteschi, A. Caneschi, M. Novak, *Nature* **1993**, *365*, 141–143.
[3] P. Gambardella, S. Stepanow, A. Dmitriev, J. Honolka, F. M. De Groot, M. Lingenfelder, S. S. Gupta, D. Sarma, P. Bencok, S. Stanescu, et al., *Nat. Mater.* **2009**, *8*, 189–193.
[4] R. Mirzoyan, R. G. Hadt, *Phys. Chem. Chem. Phys.* **2020**, *22*, 11249–11265.
[5] L. Ungur, S.-Y. Lin, J. Tang, L. F. Chibotaru, *Chem. Soc. Rev.* **2014**, *43*, 6894–6905.
[6] H. B. Heersche, Z. de Groot, J. A. Folk, H. S. J. van der Zant, C. Romeike, M. R. Wegewijs, L. Zobbi, D. Barreca, E. Tondello, A. Cornia, *Phys. Rev. Lett.* **2006**, *96*, 01.
[7] L. Bogani, W. Wernsdorfer, *Nat. Mater.* **2008**, *7*, 179–186.
[8] M. N. Leuenberger, D. Loss, *Nature* **2001**, *410*, 789–793.
[9] G. A. Timco, S. Carretta, F. Troiani, F. Tuna, R. J. Pritchard, C. A. Muryn, E. J. McInnes, A. Ghirri, A. Candini, P. Santini, et al., *Nat. Nanotechnol.* **2009**, *4*, 173.
[10] G. Aromí, D. Aguila, P. Gamez, F. Luis, O. Roubeau, *Chem. Soc. Rev.* **2012**, *41*, 537–546.
[11] A. Caneschi, D. Gatteschi, R. Sessoli, A. L. Barra, L. C. Brunel, M. Guillot, *J. Am. Chem. Soc.* **1991**, *113*, 5873–5874.
[12] F.-S. Guo, B. M. Day, Y.-C. Chen, M.-L. Tong, A. Mansikkamäki, R. A. Layfield, *Science* **2018**, *362*, 1400–1403.
[13] C. M. Zaleski, E. C. Depperman, J. W. Kampf, M. L. Kirk, V. L. Pecoraro, *Angew. Chem. Int. Ed.* **2004**, *116*, 4002–4004.
[14] S. Osa, T. Kido, N. Matsumoto, N. Re, A. Pochaba, J. Mrozinski, *J. Am. Chem. Soc.* **2004**, *126*, 420–421.
[15] N. Ahmed, C. Das, S. Vaidya, S. K. Langley, K. S. Murray, M. Shanmugam, *Chem. Eur. J.* **2014**, 14235–14239.
[16] S. K. Langley, N. F. Chilton, B. Moubaraki, K. S. Murray, *Inorg. Chem. Front.* **2015**, *2*, 867–875.
[17] E. Moreno Pineda, N. F. Chilton, F. Tuna, R. E. Winpenny, E. J. McInnes, *Inorg. Chem.* **2015**, *54*, 5930–5941.
[18] S. K. Langley, D. P. Wielechowski, N. F. Chilton, B. Moubaraki, K. S. Murray, *Inorg. Chem.* **2015**, *54*, 10497–10503.
[19] J.-L. Liu, J.-Y. Wu, G.-Z. Huang, Y.-C. Chen, J.-H. Jia, L. Ungur, L. F. Chibotaru, X.-M. Chen, M.-L. Tong, *Sci. Rep.* **2015**, *5*, 1–9.
[20] C. A. Gould, E. Mu, V. Vieru, L. E. Darago, K. Chakarawet, M. I. Gonzalez, S. Demir, J. R. Long, *J. Am. Chem. Soc.* **2020**, *142*, 21197–21209.
[21] A. A. Popov, S. M. Avdoshenko, A. M. Pendás, L. Dunsch, *Chem. Commun.* **2012**, *48*, 8031–8050.
[22] A. A. Popov, *Curr. Opin. Electrochem.* **2018**, *8*, 73–80.
[23] N. A. Samoylova, S. M. Avdoshenko, D. S. Krylov, H. R. Thompson, A. C. Kirkhorn, M. Rosenkranz, S. Schiemenz, F. Ziegs, A. U. Wolter, S. Yang, et al., *Nanoscale* **2017**, *9*, 7977–7990.
[24] Z. Wang, R. Kitaura, H. Shinohara, *J. Phys. Chem. C* **2014**, *118*, 13953–13958.
[25] W. Fu, J. Zhang, T. Fuhrer, H. Champion, K. Furukawa, T. Kato, J. E. Mahaney, B. G. Burke, K. A. Williams, K. Walker, et al., *J. Am. Chem. Soc.* **2011**, *133*, 9741–9750.
[26] T. Zuo, L. Xu, C. M. Beavers, M. M. Olmstead, W. Fu, T. D. Crawford, A. L. Balch, H. C. Dorn, *J. Am. Chem. Soc.* **2008**, *130*, 12992–12997.
[27] M. K. Singh, N. Yadav, G. Rajaraman, *Chem. Commun.* **2015**, *51*, 17732–17735.
[28] G. Velkos, D. Krylov, K. Kirkpatrick, X. Liu, L. Spree, A. Wolter, B. Büchner, H. Dorn, A. Popov, *Chem. Commun.* **2018**, *54*, 2902–2905.
[29] Z. Hu, B.-W. Dong, Z. Liu, J.-J. Liu, J. Su, C. Yu, J. Xiong, D.-E. Shi, Y. Wang, B.-W. Wang, et al., *J. Am. Chem. Soc.* **2018**, *140*, 1123–1130.
[30] G. Velkos, D. S. Krylov, K. Kirkpatrick, L. Spree, V. Dubrovin, B. Büchner, S. M. Avdoshenko, V. Bezmelnitsyn, S. Davis, P. Faust, et al., *Angew. Chem. Int. Ed.* **2019**, *58*, 5891–5896; *Angew. Chem.* **2019**, *131*, 5951–5956.
[31] L. Spree, F. Liu, V. Neu, M. Rosenkranz, G. Velkos, Y. Wang, S. Schiemenz, J. Dreiser, P. Gargiani, M. Valvidares, et al., *Adv. Funct. Mater.* **2021**, *31*, 2105516.
[32] S. A. Sulway, R. A. Layfield, F. Tuna, W. Wernsdorfer, R. E. Winpenny, *Chem. Commun.* **2012**, *48*, 1508–1510.
[33] R. J. Blagg, L. Ungur, F. Tuna, J. Speak, P. Comar, D. Collison, W. Wernsdorfer, E. J. McInnes, L. F. Chibotaru, R. E. Winpenny, *Nat. Chem.* **2013**, *5*, 673–678.
[34] E. M. Pineda, Y. Lan, O. Fuhr, W. Wernsdorfer, M. Ruben, *Chem. Sci.* **2017**, *8*, 1178–1185.
[35] J. Wang, Q.-W. Li, S.-G. Wu, Y.-C. Chen, R.-C. Wan, G. Z. Huang, Y. Liu, J.-L. Liu, D. Reta, M. J. Giansiracusa, et al., *Angew. Chem. Int. Ed.* **2021**, *60*, 5299–5306; *Angew. Chem.* **2021**, *133*, 5359–5366.
[36] S. Demir, J. M. Zadrozny, M. Nippe, J. R. Long, *J. Am. Chem. Soc.* **2012**, *134*, 18546–18549.
[37] B. S. Dolinar, S. Gómez-Coca, D. I. Alexandropoulos, K. R. Dunbar, *Chem. Commun.* **2017**, *53*, 2283–2286.
[38] C. A. Gould, L. E. Darago, M. I. Gonzalez, S. Demir, J. R. Long, *Angew. Chem. Int. Ed.* **2017**, *56*, 10103–10107; *Angew. Chem.* **2017**, *129*, 10237–10241.
[39] M. A. Dunstan, E. Rousset, M.-E. Boulon, R. W. Gable, L. Sorace, C. Boskovic, *Dalton Trans.* **2017**, *46*, 13756–13767.
[40] P. Zhang, M. Perfetti, M. Kern, P. P. Hallmen, L. Ungur, S. Lenz, M. R. Ringenberg, W. Frey, H. Stoll, G. Rauhut, J. van Slageren, *Chem. Sci.* **2018**, *9*, 1221–1230.
[41] W. R. Reed, M. A. Dunstan, R. W. Gable, W. Phonsri, K. S. Murray, R. A. Mole, C. Boskovic, *Dalton Trans.* **2019**, *48*, 15635–15645.
[42] S. Demir, I.-R. Jeon, J. R. Long, T. D. Harris, *Coord. Chem. Rev.* **2015**, *289–290*, 149–176.
[43] U. Albold, H. Bamberger, P. P. Hallmen, J. van Slageren, B. Sarkar, *Angew. Chem. Int. Ed.* **2019**, *58*, 9802–9806; *Angew. Chem.* **2019**, *131*, 9907–9911.
[44] M. A. Hay, C. Boskovic, *Chem. Eur. J.* **2021**, *27*, 3608–3637.
[45] A. E. Thorarinsdottir, R. Bjornsson, T. D. Harris, *Inorg. Chem.* **2020**, *59*, 4634–4649.
[46] N. Mavragani, D. Errulat, D. A. Gálico, A. A. Kitos, A. Mansikkamäki, M. Murugesu, *Angew. Chem. Int. Ed.* **2021**, *60*, 24206–24213.
[47] J. D. Rinehart, J. R. Long, *Chem. Sci.* **2011**, *2*, 2078–2085.
[48] J. D. Rinehart, M. Fang, W. J. Evans, J. R. Long, *J. Am. Chem. Soc.* **2011**, *133*, 14236–14239.
[49] V. Vieru, N. Iwahara, L. Ungur, L. F. Chibotaru, *Sci. Rep.* **2016**, *6*, 24046.
[50] S. Demir, M. I. Gonzalez, L. E. Darago, W. J. Evans, J. R. Long, *Nat. Commun.* **2017**, *8*, 1–9.
[51] B. M. Day, F.-S. Guo, R. A. Layfield, *Acc. Chem. Res.* **2018**, *51*, 1880–1889.
[52] G. T. Nguyen, L. Ungur, *Phys. Chem. Chem. Phys.* **2021**, *23*, 10303–10310.
[53] L. Ungur, L. F. Chibotaru, *Chem. Eur. J.* **2017**, *23*, 3708–3718.
[54] L. Ungur, L. F. Chibotaru, *Inorg. Chem.* **2016**, *55*, 10043–10056.
[55] N. Iwahara, L. F. Chibotaru, *Phys. Rev. B* **2015**, *91*, 174438.
[56] F. Liu, D. S. Krylov, L. Spree, S. M. Avdoshenko, N. A. Samoylova, M. Rosenkranz, A. Kostanyan, T. Greber, A. U. Wolter, B. Büchner, et al., *Nat. Commun.* **2017**, *8*, 1–9.
[57] N. Iwahara, Z. Huang, I. Neefjes, L. F. Chibotaru, *arXiv e-prints*, 2020, arXiv:2011.09626.
[58] F. Liu, D. S. Krylov, L. Spree, S. M. Avdoshenko, N. A. Samoylova, M. Rosenkranz, A. Kostanyan, T. Greber, A. U. Wolter, B. Büchner, et al., *Nat. Commun.* **2017**, *8*, 1–9.
[59] S. Dey, G. Rajaraman, *Chem. Sci.* **2021**, *12*, 14207–14216.
[60] C. A. Gould, K. R. McClain, D. Reta, J. G. Kragskow, D. A. Marchiori, E. Lachman, E.-S. Choi, J. G. Analytis, R. D. Britt, N. F. Chilton, et al., *Science* **2022**, *375*, 198–202.

[61] I. Fdez Galvan, M. Vacher, A. Alavi, C. Angeli, F. Aquilante, J. Autschbach, J. J. Bao, S. I. Bokarev, N. A. Bogdanov, R. K. Carlson, L. F. Chibotaru, J. Creutzberg, N. Dattani, M. G. Delcey, S. S. Dong, A. Dreuw, L. Freitag, L. M. Frutos, L. Gagliardi, F. Gendron, A. Giussani, L. Gonzalez, G. Grell, M. Guo, C. E. Hoyer, M. Johansson, S. Keller, S. Knecht, G. Kovacevic, E. Kallman, G. Li Manni, M. Lundberg, Y. Ma, S. Mai, J. P. Malhado, P. A. Malmqvist, P. Marquetand, S. A. Mewes, J. Norell, M. Olivucci, M. Oppel, Q. M. Phung, K. Pierloot, F. Plasser, M. Reiher, A. M. Sand, I. Schapiro, P. Sharma, C. J. Stein, L. K. Sorensen, D. G. Truhlar, M. Ugandi, L. Ungur, A. Valentini, S. Vancoillie, V. Veryazov, O. Weser, T. A. Wesolowski, P.-O. Widmark, S. Wouters, A. Zech, J. P. Zobel, R. Lindh, *J. Chem. Theory Comput.* **2019**, *15*, 5925–5964.
[62] F. Aquilante, J. Autschbach, R. K. Carlson, L. F. Chibotaru, M. G. Delcey, L. De Vico, I. Fdez Galvan, N. Ferre, L. M. Frutos, L. Gagliardi, M. Garavelli, A. Giussani, C. E. Hoyer, G. Li Manni, H. Lischka, D. Ma, P. A. Malmqvist, T. Muller, A. Nenov, M. Olivucci, T. B. Pedersen, D. Peng, F. Plasser, B. Pritchard, M. Reiher, I. Rivalta, I. Schapiro, J. Segarra-Marti, M. Stenrup, D. G. Truhlar, L. Ungur, A. Valentini, S. Vancoillie, V. Veryazov, V. P. Vysotskiy, O. Weingart, F. Zapata, R. Lindh, *J. Comput. Chem.* **2016**, *37*, 506–541.
[63] B. O. Roos, R. Lindh, P.-A. Malmqvist, V. Veryazov, P.-O. Widmark, A. C. Borin, *J. Phys. Chem. A* **2008**, *112*, 11431–11435.
[64] P. A. Malmqvist, B. O. Roos, B. Schimmelpfennig, *Chem. Phys. Lett.* **2002**, *357*, 230–240.
[65] L. F. Chibotaru, L. Ungur, *J. Chem. Phys.* **2012**, *137*, 064112.
[66] "Ab Initio Methodology for Pseudospin Hamiltonians of Anisotropic Magnetic Complexes", L. F. Chibotaru in *Advances in Chemical Physics, Vol. 153* (Eds.: S. A. Rice, A. R. Dinner), Wiley, **2013**, pp. 397–519.
[67] "Computational Modelling of the Magnetic Properties of Lanthanide Compounds", L. Ungur, L. F. Chibotaru in *Lanthanides and Actinides in Molecular Magnetism* (Eds.: R. A. Layfield, M. Murugesu), Wiley-VCH, **2015**, pp. 153–184.
[68] L. Chibotaru, *Structure and Bonding* **2014**, *164*, 185–230.
[69] L. F. Chibotaru, L. Ungur, *The computer programs SINGLE_ANISO and POLY_ANISO*, University of Leuven, **2006**.

Manuscript received: January 22, 2022
Version of record online: April 13, 2022